Trees (2016) 30:305–316
DOI 10.1007/s00468-015-1302-4

ORIGINAL ARTICLE

Freezing xylem conduits with liquid nitrogen creates artifactual embolisms in water-stressed broadleaf trees

Toshihiro Umebayashi[1,2] · Mayumi Y. Ogasa[1,3] · Naoko H. Miki[4] · Yasuhiro Utsumi[5] · Tomoyuki Haishi[6] · Kenji Fukuda[1]

Received: 19 June 2015 / Revised: 13 September 2015 / Accepted: 22 September 2015 / Published online: 3 October 2015

Abstract

Key message **Freezing with liquid nitrogen promotes the expansion of air in water columns of water-stressed, intact trees that are not transpiring.**

Abstract In analyses of the distribution of water-filled and embolized conduits, xylem sap is frozen with liquid nitrogen and visualized using cryo-scanning electron microscopy (cryo-SEM). However, artifacts may be introduced during preparation of samples for these analyses. If the xylem is frozen intact, conduits may embolize during freezing when xylem water potential (Ψ_{xylem}) is substantially negative, whereas rehydration to release negative pressure may induce artifactual refilling. To evaluate these sampling phenomena during dehydration and rehydration, we monitored dynamic changes in xylem functional status in the stem of *Dendropanax trifidus* by compact magnetic resonance imaging (CMRI). We also visualized the water distribution in xylem (under low Ψ_{xylem} and with no transpiration) after freezing *D. trifidus* and *Carpinus tschonoskii* stems with liquid nitrogen. Artifactual refilling of embolized conduits was sometimes observed in *D. trifidus* samples cut underwater prior to freezing; however, the extent of refilling may have no influence on hydraulic measurements. Living cells in all samples were dramatically restored after rehydration by cutting underwater. In the current-year xylem, intact saplings of *C. tschonoskii* frozen with liquid nitrogen after dehydration had a greater number of embolized vessels than samples cut underwater. When a low Ψ_{xylem} (≤ -2.5 MPa) was maintained, artifactual embolisms were rarely observed in samples directly frozen after rehydration. Thus, relaxation of negative Ψ_{xylem} and rehydration are important factors for consideration when assessing the distribution of embolized conduits by cryo-SEM.

Keywords Water stress · Embolism · *Dendropanax trifidus* · *Carpinus tschonoskii* · Cryo-SEM · CMRI

Communicated by M. Zwieniecki.

✉ Toshihiro Umebayashi
toshiumebayashi@gmail.com

[1] Laboratory of Evaluation of Natural Environment, Department of Natural Environmental Studies, Graduate School of Frontier Sciences, The University of Tokyo, Kashiwa, Japan

[2] Research Faculty of Agriculture, Hokkaido University, Sapporo, Japan

[3] Department of Plant Ecology, Forestry and Forest Products Research Institute, Tsukuba, Japan

[4] Graduate School of Environmental and Life Science, Okayama University, Okayama, Japan

[5] Asyoro Research Forest, Kyushu University, Asyoro, Japan

[6] MRTechnology Inc., Tsukuba, Japan

Introduction

Gas bubbles can form as water freezes. The appearance of bubbles is a potential threat to the xylem water-conducting system of plants. Freezing of sap usually happens during the winter season in sub-zero climates and induces cavitation (i.e., breakage of the water column) through the expansion of bubbles upon thawing (Tyree and Sperry 1989; Utsumi et al. 1999; Mayr and Sperry 2010). The likelihood of freeze–thaw-induced embolisms increases with conduit diameter (Davis et al. 1999; Pittermann and Sperry 2003, 2006) and the number of freeze–thaw cycles (Mayr et al. 2003, 2007). Furthermore, the frequency of

cavitations increases during periods of elevated negative xylem water potential (Ψ_{xylem}) during thawing; thus, even plants with narrow conduits become vulnerable when thaw pressures are sufficiently low (Mayr and Sperry 2010). Because of these relationships, conifers with narrow tracheids that are ordinarily very resistant to freeze–thaw-induced cavitation become vulnerable when they are water deficient (Pittermann and Sperry 2006). Hence, all woody plants growing at high latitudes or elevations are potentially susceptible to freeze–thaw-induced cavitation (Mayr et al. 2003).

Artificially freezing sap is also a potentially useful means of identifying and capturing images of the distribution of water-filled xylem conduits, but only so long as the freezing does not cause artifactual cavitation prior to imaging. Although the non-destructive methods such as magnetic resonance imaging (MRI) and X-ray tomography are very effective tools for the observation of liquid water distribution in plants, the use of these methods is limited in small samples such as the cut branches and potted plants in the laboratory (e.g., Holbrook et al. 2001; Utsuzawa et al. 2005; Brodersen et al. 2013). Cryo-scanning electron microscopy (cryo-SEM) is utilized for observing the in situ distribution of water-filled conduits and xylem structures at the cellular level in plants of relatively large sizes growing in the field (Utsumi et al. 1996; Canny 1997; Kuroda et al. 2009). Utsumi et al. (1999) rapidly froze xylem sap with liquid nitrogen, and then used cryo-SEM to identify the accumulation of embolisms in large earlywood vessels of the current year in a ring-porous species following a sequence of natural freeze–thaw cycles. All manipulations were performed on well-watered plants after leaf fall; hence, no transpiration occurred during liquid nitrogen freezing, and no strong negative pressures developed. Therefore, liquid nitrogen freezing itself did not cause embolisms, as indicated by the ice filling in all vessels examined by cryo-SEM prior to any natural frost. Nevertheless, Cochard et al. (2000) reported that up to 30 % of xylem conduits in walnut (*Juglans regia*) petioles were embolized by liquid nitrogen freezing at midday, presumably because extremely low Ψ_{xylem} developed rapidly as ice formation impeded water flow and leaf transpiration continued pulling on the sap stream. Actually, sampling under negative Ψ_{xylem} is very sensitive to the occurrence of embolisms. It is also known that sampling under transpiration leads to an experimental artifact because of air entry into conduits upon cutting stem underwater (Wheeler et al. 2013; Trifilò et al. 2014). Thus, progress in cryo-SEM studies requires assessments of the probability of artifactual embolism caused by liquid nitrogen freezing.

Most previous studies of freeze–thaw-induced cavitation have been conducted under static, non-transpiration conditions (e.g., Davis et al. 1999; Mayr and Sperry 2010). Utsumi et al. (1996, 1998, 2003), Umebayashi et al. (2007, 2008, 2010) and Cobb et al. (2007) collected frozen samples under static, predawn conditions to evaluate the water condition of xylem conduits by cryo-SEM. Unfortunately, the extent to which negative Ψ_{xylem} under static conditions influences the outcome of liquid nitrogen freezing is as yet undetermined. Liquid nitrogen freezing of static water columns under highly negative Ψ_{xylem} has two potential outcomes that might be observed by cryo-SEM: (1) no embolism formation, because the microbubbles that appear do not expand in the sap immobilized by freezing, or (2) embolism occurs during liquid nitrogen freezing because bubbles expand under negative pressure before the liquid sap is frozen. We explored these potential responses in the xylem of plants subjected to soil water deficiency. We used potted woody plants under drought stress as experimental material and determined the xylem functional status of segments cut underwater, as recommended by Cochard et al. (2001). We note, however, that Canny et al. (2001) suggested that this sampling method entails a risk of artificially refilling embolized conduits. A natural refilling phenomenon has been observed (non-destructively) in intact plants using both MRI (Holbrook et al. 2001; Clearwater and Clark 2003) and high-resolution X-ray computed tomography (HRCT; Brodersen et al. 2010), but whether or not artifactual refilling is also induced in samples cut underwater remains unclear. In addition, many reports have examined native hydraulic conductivity based on cut segments, but the occurrence of artifactual embolisms during sampling is not well understood (Tyree and Zimmermann 2002; Sperry 2013). Thus, studies are needed to examine artificial phenomena with regard to embolisms and refilling induced in cut segments.

In this study, we visually examined the water-filled status of xylem conduits in two woody species during dehydration and rehydration (Fig. 1). We first used CMRI to non-destructively monitor (1) artifactual embolisms and (2) refilling during dehydration and rehydration in saplings of an evergreen semi-ring-porous species [*Dendropanax trifidus* (Thunb.) Makino]. The effects of liquid nitrogen freezing on dehydrated plants (under static conditions) were also assessed by monitoring the recovery of Ψ_{xylem} following re-irrigation of plants; we concurrently checked for the presence of embolisms using CMRI and cryo-SEM. We also performed experiments on a deciduous, diffuse-porous species (*Carpinus tschonoskii* Maxim.) to compare the water-filled status of intact xylem frozen with liquid nitrogen between (1) directly frozen stems and (2) those cut underwater to relax negative pressure from the same (water-stressed) sapling. Based on the distribution of vessels containing air (VCA), we determined whether artifactual

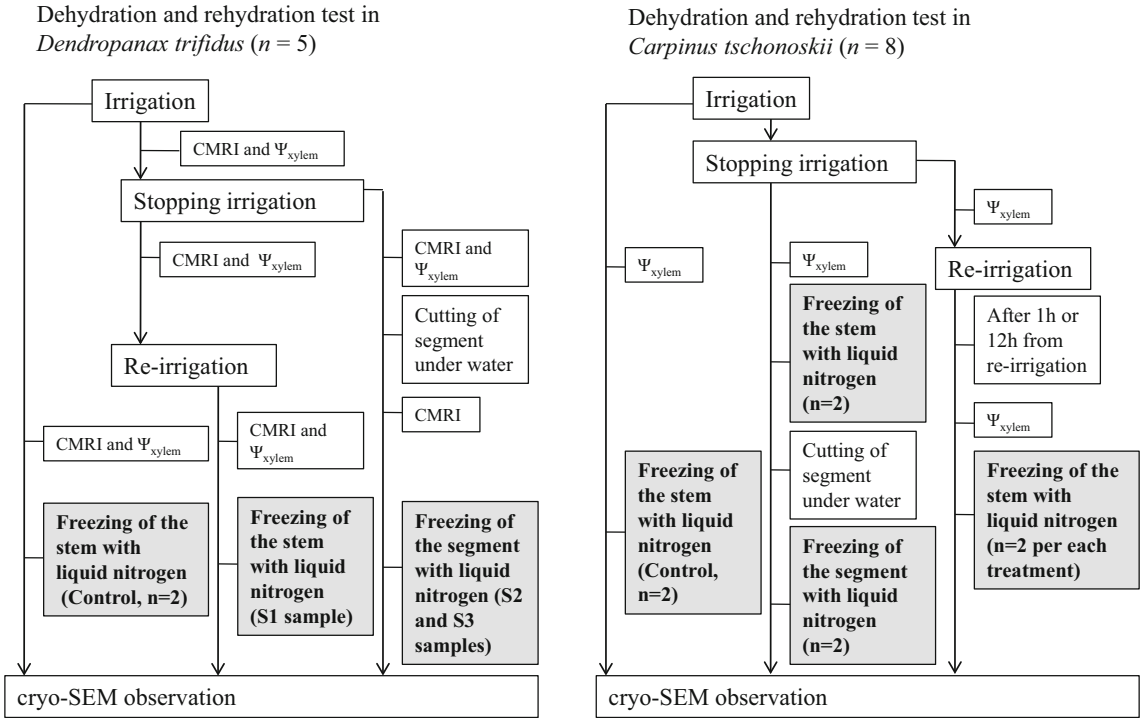

Fig. 1 A flowchart of this experiment procedure. *CMRI* visualization using compact magnetic resonance imaging, Ψ_{xylem} the measurement of xylem water potential

embolisms were induced during cutting in air and subsequent refilling. Thus, we were able to (1) determine whether (under water stress) freeze-induced bubbles expand in water frozen by liquid nitrogen, and (2) measure the frequency of artifactually embolized and refilled vessels in samples cut underwater and those cut in air.

Materials and methods

Plant materials

Experiments were conducted on potted saplings of (1) an evergreen semi-ring-porous species [*Dendropanax trifidus* (Thunb.) Makino; $n = 5$] with large earlywood vessels on the Kashiwa campus of the University of Tokyo (Kashiwa City, Chiba Prefecture, Japan) and (2) a deciduous diffuse-porous species (*Carpinus tschonoskii* Maxim.; $n = 8$) on the Tsushima campus of Okayama University (Okayama City, Okayama Prefecture, Japan). Variations in hydraulic conductivity during dehydration and rehydration of *C. tschonoskii* have been described by Ogasa et al. (2013). All saplings were well watered until experiments were initiated. *D. trifidus* saplings were 1.1 ± 0.5 m (mean ± SD) tall and 16.3 ± 9.7 mm in diameter at ground level and *C. tschonoskii* saplings were 1.3 ± 0.1 m tall and 9.8 ± 1.1 mm in diameter at ground level.

Non-destructive monitoring of xylem functional status during dehydration and rehydration

Xylem was monitored throughout August 2012. Three *D. trifidus* saplings (S1, S2, and S3) were dehydrated and rehydrated by stopping and starting irrigation, respectively (Fig. 1). Two control saplings were kept well watered. Mean Ψ_{xylem} in three leaves was measured using a pressure chamber (Model 600, PMS Instrument Co., Albany, OR, USA) in the pre-dawn before the experiment. The three experimental saplings were dehydrated until Ψ_{xylem} was ≤ -2.0 MPa. A solenoid rf probe coil (1-cm inner diameter) was fitted to sapling main stems 50 cm above ground level and a 1-mm-thick stem was monitored by CMRI. Water distribution in the main stem during dehydration was monitored regularly by CMRI.

Ψ_{xylem} in one sample (S1) decreased dramatically during dehydration (relative to the other two saplings). S1 was re-watered immediately after the decrease in Ψ_{xylem} (−3.1 MPa). The last magnetic resonance (MR) image was captured on the intact stem after near recovery to the pre-dehydration level (−0.4 MPa). We subsequently set a watertight collar to take a frozen 5-cm-long stem section including the intact monitoring location on the S1 stem. The funnel was fitted to the sample stem and the collars were filled with liquid nitrogen. To take the frozen sample, conditions were maintained for approximately 5 min. After

final monitoring during dehydration, we cut the main stems of the other two samples (S2 and S3) into 10-cm-long segments underwater. Plastic tubes filled with water were fitted to both ends of each segment and captured images by CMRI within 10 min of the final monitoring. After capturing the last MR image, samples were quickly frozen by the above protocol to freeze the monitoring location for observation of the water filling status of the xylem conduits by cryo-SEM. Following dehydration and rehydration experiments, the two control saplings were frozen directly with liquid nitrogen to visualize water distribution in intact saplings under stress-free conditions.

Analysis by CMRI

The CMRI system used in this study employed both a C-shaped modified Halbach magnet with a field strength of 1.0 T in a 25-mm air gap (Neomax Engineering Co. Ltd., Takasaki, Japan) and a portable MRI console (MRTechnology, Inc., Tsukuba, Japan) (Kose and Haishi 2011). A solenoid rf coil was wound for each imaging sample and installed in the vertical air gap of the magnet. A T_1-weighted spin-echo sequence with a repetition time (TR) of 500 ms and an echo time (TE) of 11 ms was used to visualize the water distribution in each cross-section of the sample. The two-dimensional imaging matrix was 128 × 128 pixels with isotropic voxel size. Image processing of all data was performed using Photoshop version 7.0 software (Adobe Systems, CA, USA).

We used saplings S1, S2 and S3 for measurements of the relative area of water distribution in xylem cross-sectional MR images. All images captured were converted into binary format with Photoshop. The threshold level used to divide black from white areas was set to the value at which the peak of all thermal background noise was completely within the black side (Umebayashi et al. 2011). Using ImageJ version 1.43u (http://imagej.nih.gov/ij/), we calculated the percentage loss of water-conducting area [PLA (%)] in xylem for each sapling as follows:

$$\mathrm{PLA}\,(\%) = 100 \times (1 - \text{number of white pixels in each experimental condition}/\text{number of white pixels in the initial condition})$$

Sampling frozen intact stems and stems cut to relax negative pressure

We selected six *C. tschonoskii* saplings for dehydration and rehydration experiments. Two additional saplings were used as controls to observe the water-filled status of xylem conduits when Ψ_{xylem} were near zero (Table 1). All samples were taken from the main stem. This experiment was performed from mid-July to October in 2011. Each sample was dried for approximately 1 week until the Ψ_{xylem} was close to a theoretical loss of half the hydraulic conductivity (−3.9 MPa in *C. tschonoskii*, Ogasa et al. 2013). Ψ_{xylem} measurements of all saplings were conducted regularly using a pressure chamber (Model 1000, PMS Instrument Co., Albany, OR, USA) in the branch tips. The tips were been previously enclosed and covered with a black plastic bag and aluminum foil to balance the Ψ_{xylem} between leaf and stem xylem.

Table 1 Xylem water potential (MPa, Ψ_{xylem}) measured in all samples in *Caprinus tschonoskii*

Carpinus tschonoskii	Ψ_{xylem}	
Control	−0.1	−0.1
After dehydration	−3.1	−3.3
From rehydration		
After 1 h	−2.9 (−3.5)	−2.5 (−3.4)
After 12 h	−0.2 (−3.6)	−0.2 (−3.1)

Numbers in parenthesis show the value of Ψ_{xylem} after dehydration

After dehydration, samples were collected from two locations on each of two *C. tschonoskii* saplings (upper and lower positions on the main stems) to examine the water filling status of xylem conduits in intact stems (Fig. 1). Before sampling, all saplings were placed in black plastic bags for at least 2 h to completely stop transpiration (as detailed by Ogasa et al. 2010). A plastic cup was fitted at a stem height of 15 cm and filled with liquid nitrogen for 5 min to directly freeze each stem sample after dehydration. Each stem was then cut into a 5-cm-long segment and stored immediately in liquid nitrogen. After this sample had been taken, we cut another segment with two annual rings underwater to a length of 10 cm. To avoid the formation of artificial embolisms from opened vessels [maximum vessel length = 16.7 ± 5.7 (mean ± SD) cm; $n = 3$] during cutting in air, samples subjected to this underwater cutting treatment were taken distal from the directly frozen segments. Before freezing the samples cut underwater, plastic tubes filled with 20 mM KCl solution were fitted to both ends of the segments. The middle portion of each segment was immersed in a bath filled with liquid nitrogen for 5 min, after which, segment length was immediately reduced to 5 cm.

The other saplings were fully re-watered after dehydration. At 1- and 12-h intervals after re-watering, a directly frozen segment was collected from each of the two saplings (Fig. 1). Freezing treatment was applied to intact saplings. Two controls were also collected from two samples of the directly frozen stem.

All frozen samples were transported from Okayama University to the University of Tokyo in a container packed

with dry ice; in Tokyo, samples where samples were transferred to a cold room at −27 °C.

Cryo-scanning electron microscopy (cryo-SEM)

Xylem functional status was observed in the middle of the frozen samples (i.e., the position monitored by CMRI) by cryo-SEM (JSM-6390 LV, JEOL, Tokyo, Japan). All frozen samples were cut in the cold room at −27 °C into small blocks (ca. 6 × 6 × 10 mm), each of which included part of the xylem tract from bark to pith. The transverse surface of each block was cut cleanly with the steel blade of a sliding microtome (Yamato Koki, Tokyo, Japan) to expose the cell lumina. Just after the treatment, the block was attached to a specimen holder and the holder was immersed in liquid nitrogen. Frozen samples were etched lightly and moved to the cold stage of a cryo-SEM maintained at ca. −160 °C. Secondary electron images were observed uncoated at an accelerating voltage of 3 kV.

We counted at least 100 vessels within the current-year and the previous year's annual rings to quantify the distribution of water-filled vessels in *C. tschonoskii*. Counts were made in triplicate for each sample.

In the semi-ring-porous species, the initial zone of an annual ring that contained large diameter vessels was identified as earlywood. We also identified early latewood as the younger half of the latewood, and late latewood as the remaining half (Umebayashi et al. 2010). All vessels were classified as either completely filled with water or containing air (VCA).

Results

Non-destructive monitoring of xylem functional status during dehydration and rehydration in *D. trifidus*

Mean Ψ_{xylem} at predawn were ≥−0.2 MPa in all test ($n = 3$) and control samples ($n = 2$) before the dehydration experiment. Cryo-SEM images of both control samples showed that many large earlywood vessels in current-year tissue were water-filled, whereas all large earlywood vessels in the inner annual rings were air-filled (Fig. 2a). Water also filled many wood fibers. In contrast, most latewood vessels and fibers were water-filled in all annual rings. This is similar to the xylem water distribution of this species growing under natural conditions (Umebayashi et al. 2010).

The distinctions between the inner bark, cambial zone, xylem, and pith were clear in all CMRI images (Fig. 3a, b). Before dehydration, water was distributed in the whole xylem, but during tissue dehydration we observed decreases in the occurrence of water in the inner bark, cambial zone, and xylem. In sapling S1, water occurred in the inner bark, cambial zone, and xylem when the pre-dawn Ψ_{xylem} was −0.3 MPa (Fig. 3a). At a Ψ_{xylem} of −3.1 MPa, we observed a decline in the outer layer of water-rich bark tissue (Fig. 3a, arrowhead). The percentage loss of water-conducting area (PLA) in the xylem reached 12.2 % of the pre-dehydration total. The progression of water loss in the xylem did not immediately stop following rehydration; the PLA increased to 34.3 % of the pre-dehydration total before recovery of Ψ_{xylem} (Fig. 3c, d, arrowheads). However, the water-rich layer in the inner bark and cambium zones recovered rapidly (Fig. 3a, arrowhead).

All large earlywood vessels and most wood fibers in all annual rings were empty in cryo-SEM images of the water distribution after rehydration (Fig. 2b, c), and many latewood vessels in the outermost and inner annual rings remained water-filled (Fig. 2b). Water droplets (Fig. 2b, c, arrow) were observed inside some embolized vessels.

In saplings S2 and S3, the water distribution in the xylem barely changed until a Ψ_{xylem} of −1.0 MPa had been reached; water loss in the xylem was clearly observed at −1.3 MPa in S2 and at −1.5 MPa in S3 (Fig. 3b). In these two saplings, a considerable volume of water was lost in the inner region of the xylem as drought stress increased (Fig. 3b, arrows). The PLA finally reached 42.8 % (S2) and 75.6 % (S3) of the total areas at a Ψ_{xylem} of −2.2 MPa, and water was lost from sections of the inner bark and the cambial zones (Fig. 3b, arrowhead).

The PLA difference before and after cutting decreased (i.e., refilled) by 6.1 % in S3, but the difference increased by 4.0 % in S2. The inner bark and cambial zones showed signs of rapid rehydration (Fig. 3b, arrowheads). In cryo-SEM images of the two dehydrated samples, all large earlywood vessels and most wood fibers in all annual rings were empty as well as those of S1 (Fig. 2b, d–f). Many latewood vessels were water-filled in the outermost and inner annual rings of S2 (Fig. 2d). In contrast, most early latewood vessels and some late-latewood vessels were empty in all annual rings of S3 (Fig. 2e, f), and the frequency of empty vessels was higher in those of large diameter than in those of narrow bore (Fig. 2f). Water droplets were also observed inside a range of vessels.

Variation in the xylem functional status frozen with liquid nitrogen during the dehydration and rehydration of *C. tschonoskii* plants

Ψ_{xylem} in the two controls was −0.1 MPa (Table 1). All of their vessels were water-filled (Fig. 4a), but the wood fibers were generally empty, with the exception of those near the

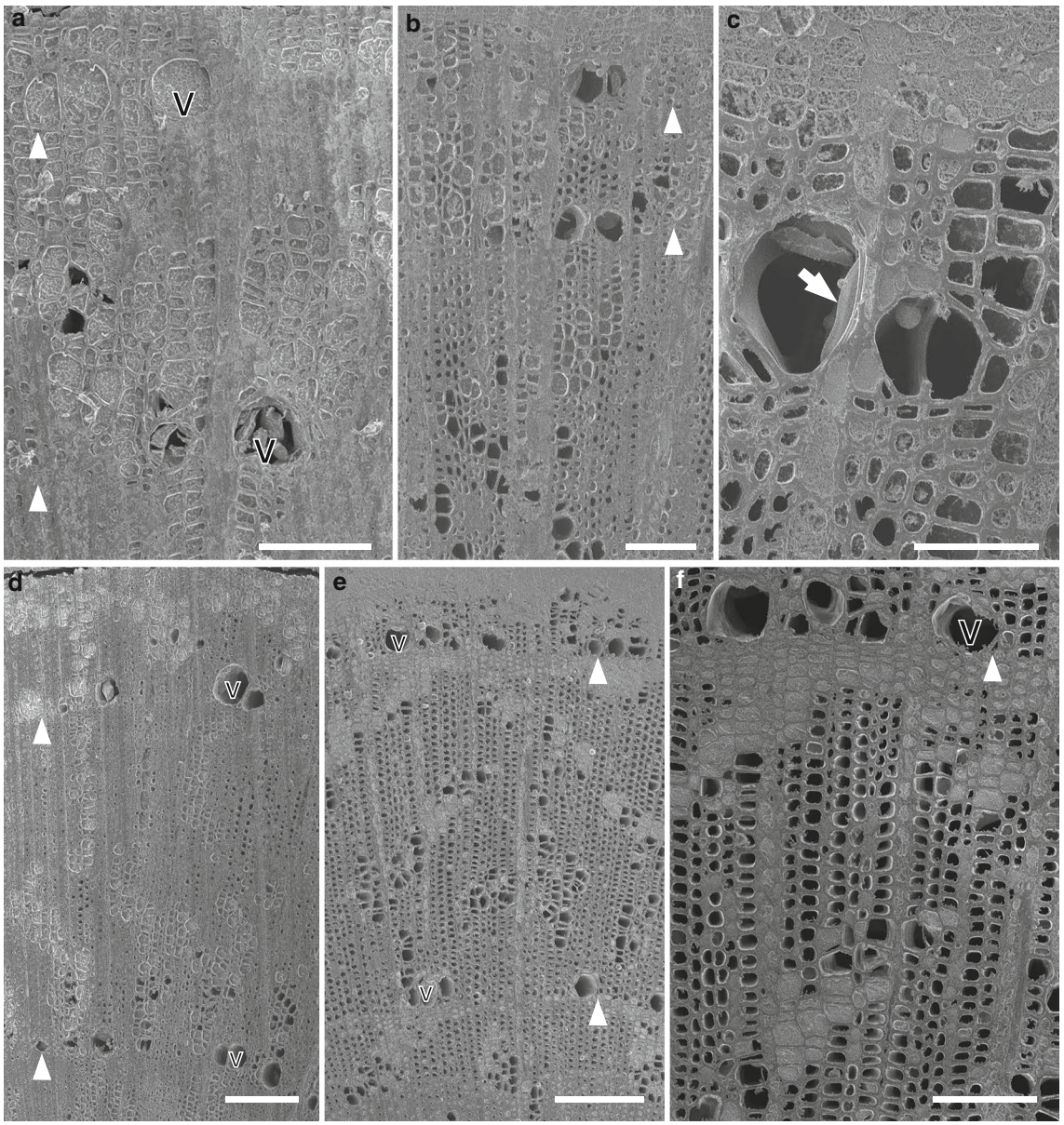

Fig. 2 Cryo-scanning electron microscopic (cryo-SEM) images of water distribution in *Dendropanax trifidus* during dehydration and rehydration. **a** Transverse surface of the outer two annual rings in the control. **b**, **c** Transverse surfaces in the outer two annual rings (**b**) and the earlywood in the outermost annual ring (**c**) of an intact stem (sapling S1) frozen after rehydration. **d** Transverse surface of the outer two annual rings in the main stem of a sapling (S2) cut under water after dehydration. **e**, **f** Transverse surfaces of the outer two annual rings (**e**) and late-latewood in the outer second annual ring (**f**) in the main stem of a sapling (S3) cut under water after dehydration. *V* large earlywood vessel, *arrowhead* annual ring, *arrow* water droplet. *Scale bars* 100 μm (**a**, **b**, **f**), 200 μm (**d**, **e**), 50 μm (**c**)

cambium. Ψ_{xylem} was −3.4 MPa after dehydration, a value close to the theoretical half loss of hydraulic conductivity (Ogasa et al. 2013). Ψ_{xylem} remained low (≤−2.5 MPa) 1 h after rehydration. Ψ_{xylem} reached −0.2 MPa after 12 h.

We categorized all vessels other than those that were completely water-filled as "vessels containing air (VCA)" (Cochard et al. 2000). During dehydration and rehydration, the proportion (%) of VCA in the current-year tissue of all samples was lower than that of previous-year tissue, and current-year values were similar among samples, except in two directly frozen stem samples subjected to dehydration (Fig. 5). During dehydration, the current-year VCA % values in samples of the directly frozen stem were clearly higher than those of samples cut underwater before freezing (Fig. 4b, c). Although the previous-year xylem VCA % values in samples of directly frozen stems were higher than those of other samples, the difference was slight (Fig. 4b–e).

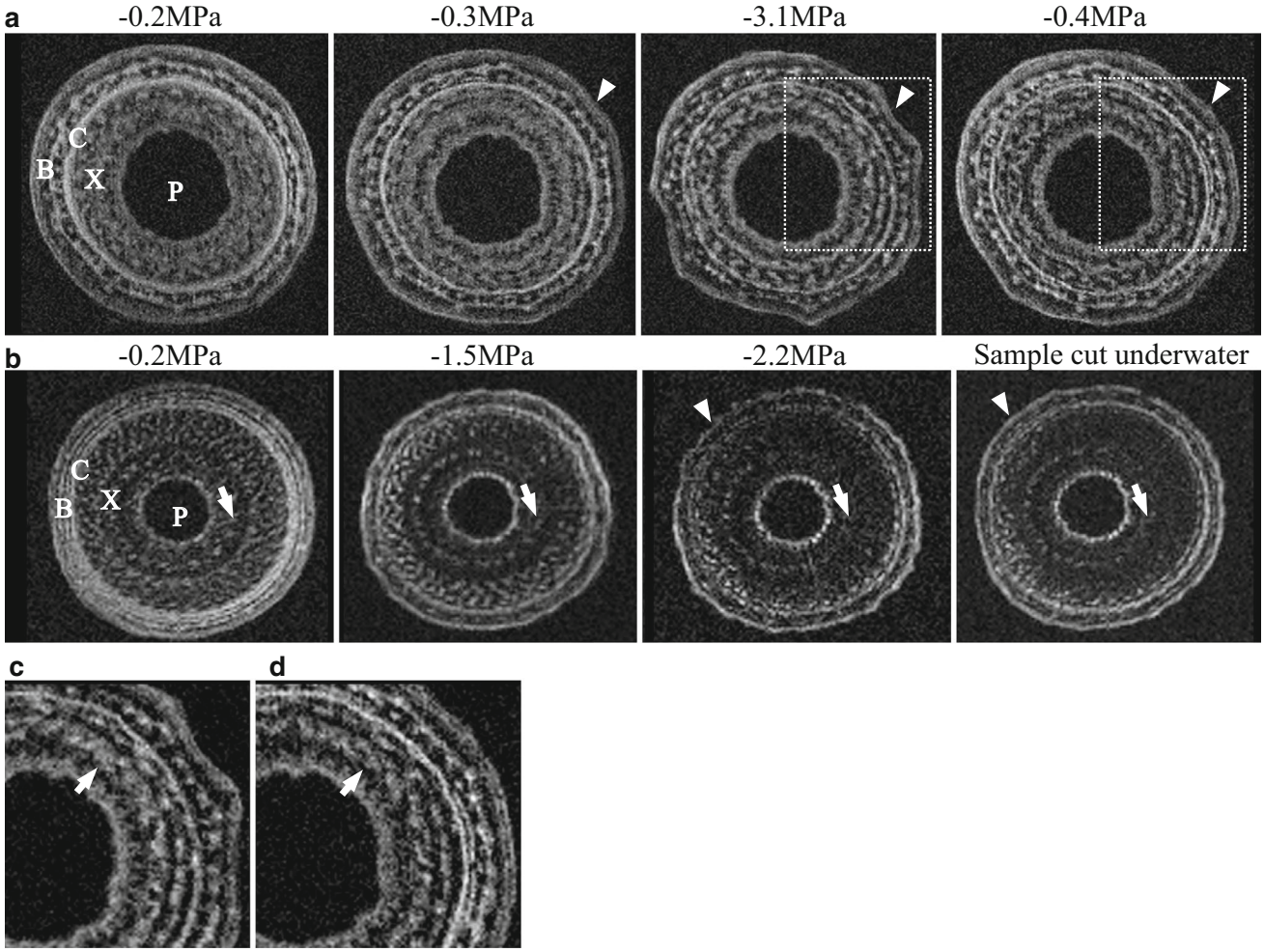

Fig. 3 Cross-sectional magnetic resonance (MR) images of the main stem of *Dendropanax trifidus* during dehydration and rehydration [compact magnetic resonance imaging (CMRI) parameters: repetition time = 500 ms, echo time = 11 ms, slice thickness in axial orientation = 1 mm]. **a** Images of water distribution in sapling S1 during dehydration and after rehydration (*B* inner bark, *C* cambial zone, *X* xylem, *P* pith). The *dotted grid* indicates the extensional regions in **c** and **d**. **b** Images of water distribution in the sample cut underwater from sapling S3 during dehydration. **c**, **d** Difference in water distribution in the xylem before and after rehydration. *Arrowheads* indicate the matching position of the water-rich layer on the inner bark. *Arrows* indicate the same position in the xylem

The distribution of air and water in VCA varied. In all samples, many of the vessels containing air were completely empty (Fig. 4). The water surface was either flat or convex in samples of directly frozen stem after dehydration, (Fig. 6a, arrows), or single, large air bubbles were positioned in the centers of the vessels (Fig. 6b, arrow). Some vessels in samples cut underwater before freezing included water and air; water droplets occurred in some vessels, (Fig. 6c, arrowheads). Many VCAs remained empty in directly frozen stems 1 and 12 h after rehydration (i.e., after re-watering), and water droplets were observed in some vessels (Fig. 6d, arrowheads).

Discussion

Water filled all vessels in control stems of *C. tschonoskii* (Fig. 4a). We observed embolized conduits after dehydration. Following dehydration, the current-year VCA % values in samples of directly frozen stem were clearly higher than those of samples cut underwater before freezing (Fig. 4b, c). Thus, the difference in values are attributable to the two different procedures used for sampling under water stress, as suggested by Cochard et al. (2000) and Canny et al. (2001). However, many embolized vessels were observed in previous-year xylem of all dehydrated samples (both directly frozen stem samples and

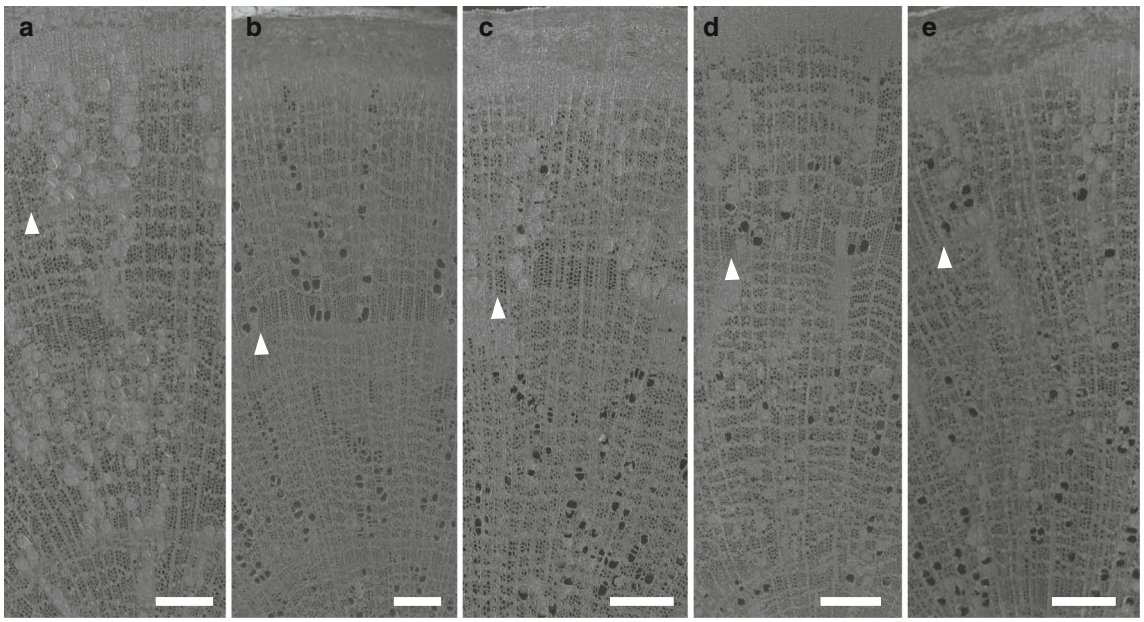

Fig. 4 Cryo-scanning electron microscopic images of water distribution in *Carpinus tschonoskii* saplings under control conditions (**a**), after dehydration (**b**, **c**), and 1 h (**d**) and 12 h (**e**) after rehydration. Transverse surfaces of the xylem in a directly frozen stem (**a**, **b**, **d**, **e**) and in a stem cut underwater (**c**). **b** and **c** are from the same sample. The *arrowheads* show the outline of an annual ring. *Scale bars* 250 µm

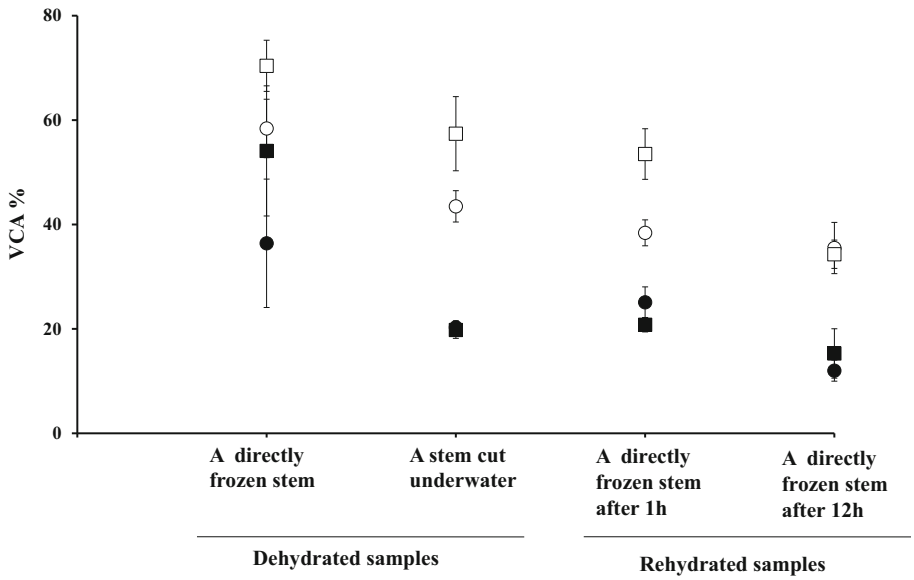

Fig. 5 Percentage of *Carpinus tschonoskii* vessels containing air (VCA %) during dehydration and rehydration. VCA % values refer to samples taken from frozen intact stems and stems cut underwater after dehydration, and from samples taken from directly frozen stems 1 and 12 h after re-irrigation. *Circles* and *squares* represent the mean VCA % value of sample (mean ± SE; $n = 3$). *Black* and *white symbols* refer to current-year and previous-year xylem, respectively

those cut underwater before freezing). Older xylem conduits are generally more vulnerable to embolisms than current-year conduits (Sperry et al. 1991). Thus, artifacts (cavitation and/or refilling) are best assessed by examining current-year xylem rather than older xylem of frozen samples subjected to water stress.

Canny et al. (2001) argued that embolized vessels in rachises of transpiring walnut leaves might rapidly refill when the xylem is cut underwater. This conclusion was based on observations of water droplets (Canny 1997). Water droplets are usually detected by cryo-SEM examination of xylem vessels in the stems of some woody plants (Utsumi et al. 1998, 1999). Refilling of embolized conduits of *Vitis* sp. has been observed at ambient pressure 1 h after the immersion of samples (Wang et al. 2013) and ca. 1 h or more after rehydration (Brodersen et al. 2010). However, the proportion of conduits that can be refilled during a short time frame of hydraulic measurements remains unknown.

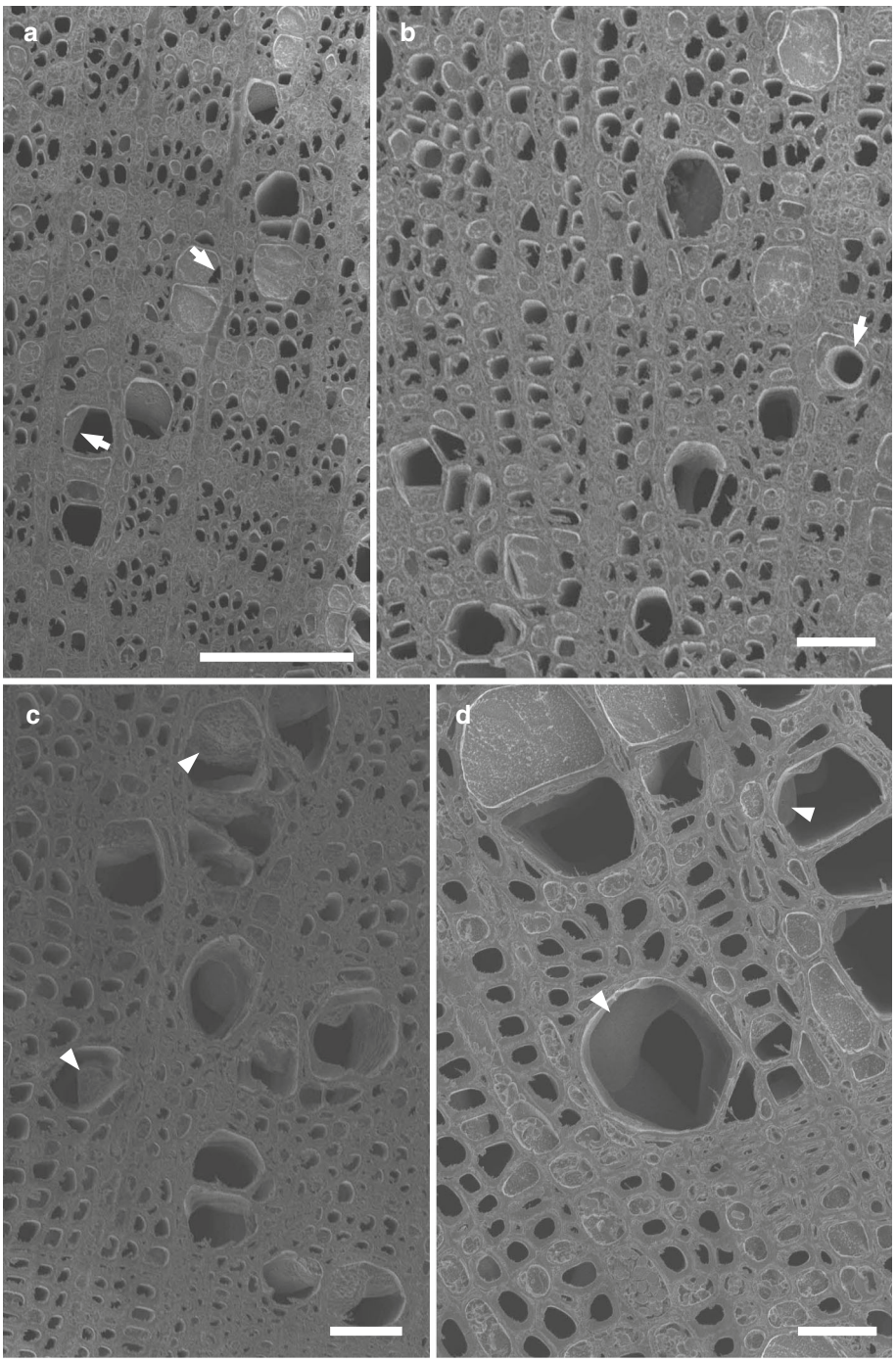

Fig. 6 Cryo-scanning electron microscopic images of water distribution in *Carpinus tschonoskii* sapling during dehydration and rehydration. **a**, **b** Transverse surfaces of current-year xylem (**a**) and previous-year xylem (**b**) in a sample taken from the directly frozen tree after dehydration. **c** Transverse surface in a sample cut underwater after dehydration. **d** Transverse surface of a sample taken from the directly frozen tree 1 h after rehydration. *Arrows* indicate the border between water and air. *Arrowheads* indicate water droplets in a conduit. *Scales bars* 200 μm (**a**), 100 μm (**b**, **c**)

We observed a few large water droplets in many samples after dehydration, and in some cases, vessels were partially filled with water (Fig. 6c, d, arrowheads). However, our CMRI monitoring of two dehydrated *D. trifidus* saplings detected very few xylem vessels refillings in stems excised under water. Furthermore, water-filled conduits were very rare in previous-year xylem of *C. tschonoskii* (Fig. 4c) and the stems of *D. trifidus* 10 min after cutting underwater. Embolisms are usually induced in open vessels when plants are cut in air. These embolisms rarely recover, even if the cut surface is rapidly immersed in water (Tyree and Zimmermann 2002). Thus, refilling is not instantaneous. We therefore conclude that refilling in sapwood is minimal immediately after cutting underwater, but whether or not water droplets contribute to the progression of refilling remains unclear.

Are embolisms induced in xylem conduits during rapid freezing of water-stressed plants with liquid nitrogen?

Water-filled vessels of all diameters occur in current-year tissue frozen when there is no transpiration flow and Ψ_{xylem} is near atmospheric (Utsumi et al. 1999). Winter embolisms occur during sap thawing (thaw-expansion hypothesis). For example, the percentage loss of conductivity (PLC) in water-stressed *Pinus contorta* increases during the thawing phase, but not during the preceding freezing phase (Mayr and Sperry 2010). Nevertheless, acoustic emissions have been detected during the freezing process in many species (Mayr et al. 2007; Mayr and Zublasing 2010; Charrier et al. 2014; Kasuga et al. 2015). Kasuga et al. (2015) indicated that cumulative numbers of acoustic emissions with absolute energy $\geq$10.0 fJ strongly correlated with the increase in PLC, and the high absolute energy of the acoustic emissions might reflect the formation of large bubbles in the large lumen of vessels. Cavitation in the vessels of angiosperms occurs when sap is frozen during transpiration (Cochard et al. 2000) or when water stress is significant, as in our study. Thus, the distribution of VCA in Fig. 4b, c may indicate that bubble expansion in the water column occurred when a vessel under critical negative pressure was frozen with liquid nitrogen. The sizes and positions of air inclusions in embolized vessels varied among vessels of similar diameter (Fig. 6a, b, arrows). Observations such as these may be specific to xylem frozen by liquid nitrogen.

Both the volume of water in each vessel and the freezing rate may vary following dehydration. We measured VCA % values in directly frozen stem samples of *C. tschonoskii* samples 1 h after rehydration that were similar to post-dehydration values of samples cut underwater before freezing, even though Ψ_{xylem} was below −2 MPa (Table 1; Fig. 5). Cochard et al. (2000) reported that in walnut petioles the VCA % values in directly frozen stems dramatically increased by up to 30 % with increasing transpiration pull (minimum −0.7 MPa); however, only water-filled vessels were observed in samples frozen in the early morning (ca. −0.25 MPa). We showed that the appearance of VCA differed markedly between flowing and close to static conditions after rehydration. Thus, information on Ψ_{xylem} and the water status of living cells is crucial for identifying the effects of freezing sap with liquid nitrogen. The water status of all living tissues may change dramatically between dehydration and rehydration (Fig. 3), and water volume probably has a very important influence on cooling progression in xylem water during freezing with liquid nitrogen.

In large earlywood vessels of the current year in a deciduous ring-porous species, *Quercus gambelii*, it is thought that the cycle between embolisms at midday and the refilling at midnight is repeated during growth season (Taneda and Sperry 2008). Although we observed many water droplets in embolized vessels in both species after rehydration (Figs. 2c, 6d), none of the large vessels or fibers in the current-year earlywood xylem of *D. trifidus* were refilled (Fig. 2b, d, e). This means that the function of large vessels may be different among species. On the other hand, several vessels of the last-year xylem in *C. tschonoskii* were a few refilled after 12 h from rehydration (Fig. 5). Ogasa et al. (2013) also reported the limited recovery of hydraulic conductivity in this diffuse-porous species after 12 h from rehydration, and our results indicated that the recovery might occur by the refilling of several embolized vessels in the last-year xylem. The underlying reason for differences in refilling between species should be determined in future studies.

We also observed large increases in the water content of living cells after rehydration; cells in the cambium and inner bark rapidly absorbed water following re-supply (Fig. 3). Samples dehydrated by the centrifugal method absorb water during measurements of hydraulic conductivity, and the water content of samples tends to increase after such measurements. Unfortunately, we were unable to monitor the dynamic status of water in the xylem parenchyma using CMRI, but it is reasonable to propose that this tissue also absorbed water. We did not investigate the process of water loss or absorption in living cells under water deficit stress, but the water content of such cells may influence resistance to cavitation in conduits and recovery from embolism.

In conclusion, when the stems of dehydrated plants were cut underwater, immediate refilling was minimal. In contrast, expansion of air bubbles in sap occurred during liquid nitrogen freezing of dehydrated samples, which is a serious confounding issue for cryo-SEM observations. Therefore, treatment to relax sample Ψ_{xylem} contributes to reliable determinations of the water-filled status of xylem conduits under drought stress (Cochard et al. 2001). The xylem cell water status of dehydrated samples influences stable freezing progression during liquid nitrogen treatment. Future studies should determine water distributions after relaxation of negative pressure and after rehydration. With a robust understanding of the constraints, cryo-SEM may be proved to be the most effective tool for observing the cell water-fill status of plants of relatively large sizes growing in the field.

Author contribution statement T.U. contributed to total construction of this study, and all data collections except for the sample freezing with liquid nitrogen during the dehydration and rehydration of *Carpinus tschonoskii* plants. M.Y.O. and N.H.M. contributed to take samples frozen with liquid nitrogen during the dehydration and rehydration of *C. tschonoskii* plants, and were involved in discussions about this study. T.H. contributed to take fine MR images. Y.U. and K.F. offered many important suggestions on this study. This study is conducted by funds awarded to K.F.

Acknowledgments This work was supported by a Grant-in Aid for Scientific Research [A] (no. 23248022). We thank John Sperry and Duncan Smith for useful comments on a first draft of our manuscript. We also thank Yuki Murakami, Okayama University, Japan, for technical support, and Kazuma Togashi, MRTechnology Inc., Japan for support in constructing and testing the MRI apparatus.

Compliance with ethical standards

Conflict of interest The authors declare that they have no conflict of interest.

References

Brodersen CR, McElrone AJ, Choat B, Matthews MA, Shackel KA (2010) The dynamics of embolism repair in xylem: in vivo visualizations using high-resolution computed tomography. Plant Physiol 154:1088–1095

Brodersen CR, McElrone AJ, Choat B, Lee EF, Shackel KA, Matthews MA (2013) In vivo visualizations of drought-induced embolism spread in *Vitis vinifera*. Plant Physiol 161:1820–1829

Canny MJ (1997) Vessel contents during transpiration–embolisms and refilling. Am J Bot 84:1223–1230

Canny MJ, McCully ME, Huang CX (2001) Cryo-scanning electron microscopy observations of vessel content during transpiration in walnut petioles. Facts or artifacts? Plant Physiol Biochem 39:555–563

Charrier G, Charra-Vaskou K, Kasuga J, Cochard H, Mayr S, Améglio T (2014) Freeze-thaw stress: effects of temperature on hydraulic conductivity and ultrasonic activity in ten woody angiosperms. Plant Physiol 164:992–998

Clearwater MJ, Clark CJ (2003) In vivo magnetic resonance imaging of xylem vessel contents in woody lianas. Plant Cell Environ 26:1205–1214

Cobb AR, Choat B, Holbrook NM (2007) Dynamics of freeze-thaw embolism in *Smilax rotundifolia* (Smilacaceae). Am J Bot 94:640–649

Cochard H, Bodet C, Améglio T, Cruiziat P (2000) Cryo-scanning electron microscopy observations of vessel content during transpiration in walnut petioles. Fact or artifacts? Plant Physiol 124:1191–1202

Cochard H, Améglio T, Cruiziat P (2001) The cohesion theory debate continues. Trends Plant Sci 6:456

Davis SD, Sperry JS, Hacke UG (1999) The relationship between xylem conduit diameter and cavitation caused by freezing. Am J Bot 86:1367–1372

Holbrook NM, Ahrens ET, Burns MJ, Zwieniecki MA (2001) In vivo observation of cavitation and embolism repair using magnetic resonance imaging. Plant Physiol 126:27–31

Kasuga J, Charrier G, Uemura M, Améglio T (2015) Characteristics of ultrasonic acoustic emissions from walnut branches during freeze-thaw-induced embolism formation. J Exp Bot 66:1965–1975

Kose K, Haishi T (2011) High resolution NMR imaging using a high field yokeless permanent magnet. Magn Reson Med Sci 10:159–167

Kuroda K, Yamashita K, Fujiwara T (2009) Cellular level observation of water loss and the refilling of tracheids in the xylem of *Cryptomeria japonica* during heartwood formation. Trees 23:1163–1172

Mayr S, Sperry JS (2010) Freeze–thaw-induced embolism in *Pinus contorta*: centrifuge experiments validate the 'thaw-expansion hypothesis' but conflict with ultrasonic emission data. New Phytol 185:1016–1024

Mayr S, Zublasing V (2010) Ultrasonic emissions from conifer xylem exposed to repeated freezing. J Plant Physiol 167:34–40

Mayr S, Schwienbacher F, Bauer H (2003) Winter at the alpine timberline. Why does embolism occur in Norway spruce but not in stone pine? Plant Physiol 131:780–792

Mayr S, Cochard H, Améglio T, Kikuta SB (2007) Embolism formation during freezing in the wood of *Picea abies*. Plant Physiol 143:60–67

Ogasa M, Miki N, Yoshikawa K (2010) Changes of hydraulic conductivity during dehydration and rehydration in *Quercus serrata* Thunb. and *Betula platyphylla* var. *japonica* Hara: the effect of xylem structures. Tree Physiol 30:608–617

Ogasa M, Miki NH, Murakami Y, Yoshikawa K (2013) Recovery performance in xylem hydraulic conductivity is correlated with cavitation resistance for temperate deciduous tree species. Tree Physiol 33:335–344

Pittermann J, Sperry J (2003) Tracheid diameter is the key trait determining the extent of freezing-induced embolism in conifers. Tree Physiol 23:907–914

Pittermann J, Sperry JS (2006) Analysis of freeze–thaw embolism in conifers. The interaction between cavitation pressure and tracheid size. Plant Physiol 140:374–382

Sperry J (2013) Cutting-edge research or cutting-edge artifact? An overdue control experiment complicates the xylem refilling story. Plant Cell Environ 36:1916–1918

Sperry JS, Perry AH, Sullivan JEM (1991) Pit membrane degradation and air-embolism formation in ageing xylem vessels of *Populus tremuloides* Michx. J Exp Bot 42:1399–1406

Taneda H, Sperry JS (2008) A case-study of water transport in co-occurring ring- versus diffuse-porous trees: contrasts in water-status, conducting capacity, cavitation and vessel refilling. Tree Physiol 28:1641–1651

Trifilò P, Raimondo F, Lo Gullo MA, Barbera PM, Salleo S, Nardini A (2014) Relax and refill: xylem rehydration prior to hydraulic measurements favours embolism repair in stems and generates artificially low PLC values. Plant Cell Environ 37:2491–2499

Tyree MT, Sperry JS (1989) Vulnerability of xylem to cavitation and embolism. Annu Rev Plant Phys Mol Biol 40:19–38

Tyree MT, Zimmermann MH (2002) Xylem structure and ascent of sap, 2nd edn. Springer, Berlin

Umebayashi T, Utsumi Y, Koga S, Inoue S, Shiiba Y, Arakawa K, Matsumura J, Oda K (2007) Optimal conditions for visualizing water-conducting pathways in a living tree by the dye injection method. Tree Physiol 27:993–999

Umebayashi T, Utsumi Y, Koga S, Inoue S, Fujikawa S, Arakawa K, Matsumura J, Oda K (2008) Conducting pathways in north temperate deciduous broadleaved trees. IAWA J 29:247–263

Umebayashi T, Utsumi Y, Koga S, Inoue S, Matsumura J, Oda K, Fujikawa S, Arakawa K, Otsuki K (2010) Xylem water-conducting patterns of 34 broadleaved evergreen trees in southern Japan. Trees 24:571–583

Umebayashi T, Fukuda K, Haishi T, Sotooka R, Zuhair S, Otsuki K (2011) The developmental process of xylem embolisms in pine wilt disease monitored by multipoint imaging using compact magnetic resonance imaging. Plant Physiol 156:943–951

Utsumi Y, Sano Y, Ohtani J, Fujikawa S (1996) Seasonal changes in the distribution of water in the outer growth rings of *Fraxinus mandshurica* var. *japonica*: a study by cryo-scanning electron microscopy. IAWA J 17:113–124

Utsumi Y, Sano Y, Fujikawa S, Funada R, Ohtani J (1998) Visualization of cavitated vessels in winter and refilled vessels in spring in diffuse-porous trees by cryo-scanning electron microscopy. Plant Physiol 117:1463–1471

Utsumi Y, Sano Y, Funada R, Fujikawa S, Ohtani J (1999) The progression of cavitation in earlywood vessels of *Fraxinus*

mandshurica var *japonica* during freezing and thawing. Plant Physiol 121:897–904

Utsumi Y, Sano Y, Funada R, Ohtani J, Fujikawa S (2003) Seasonal and perennial changes in the distribution of water in the sapwood of conifers in a sub-frigid zone. Plant Physiol 131:1826–1833

Utsuzawa S, Fukuda K, Sakaue D (2005) Use of magnetic resonance microscopy for the nondestructive observation of xylem cavitation caused by pine wilt disease. Phytopathology 95:737–743

Wang M, Tyree MT, Wasylishen RE (2013) Magnetic resonance imaging of water ascent in embolized xylem vessels of grapevine stem segments. Can J Plant Sci 93:879–893

Wheeler JK, Huggett BA, Tofte AN, Rockwell FE, Holbrook NM (2013) Cutting xylem under tension or supersaturated with gas can generate PLC and the appearance of rapid recovery from embolism. Plant Cell Environ 36:1938–1949